Catalysis Science & Technology

Accepted Manuscript

This article can be cited before page numbers have been issued, to do this please use: Md. R. Sarkar and S. G. Bell, *Catal. Sci. Technol.*, 2020, DOI: 10.1039/D0CY01040E.

ROYAL SOCIETY OF CHEMISTRY

rsc.li/catalysis

View Article Online
DOI: 10.1039/D0CY01040E

ARTICLE

Complementary and selective oxidation of hydrocarbon derivatives by two cytochrome P450 enzymes of the same family

Md. Raihan Sarkar[a] and Stephen G. Bell*,

Received 00th January 20xx,
Accepted 00th January 20xx

DOI: 10.1039/x0xx00000x

The cytochrome P450 enzymes CYP101B1 and CYP101C1, which are from the bacterium *Novosphingobium aromaticivorans* DSM12444, can hydroxylate norisoprenoids with high activity and selectivity. With the goal of expanding and establishing their substrate range with a view to developing applications, the oxidation of a selection of cyclic alkanes, ketones and alcohols was investigated. Cycloalkanes were oxidised, but both enzymes displayed moderate binding affinity and low levels of productive activity. We improved the binding and activity of these substrates with CYP101B1 by making the active site more hydrophobic by switching a histidine residue to a phenylalanine (H85F). The presence of a ketone moiety in the cycloalkane skeleton significantly improved the oxidation activity with both enzymes. CYP101C1 preferably catalysed the oxidation of cycloalkanones at the C-2 position whereas CYP101B1 oxidised these substrates with higher productivity and at positions remote from the carbonyl group. This demonstrates that the binding orientation of the cyclic ketones in the active site of each enzyme must be different. Linear ketones were also oxidised by both enzymes but with lower activity and selectivity. Cyclic substrates with an ester directing group were more efficiently oxidised by CYP101B1 than CYP101C1. Both enzymes catalysed oxidation of these esters with high regioselectively on the ring system remote from the ester directing group. CYP101C1 selectively oxidised certain terpenoid ester substrates, such as *α*-terpinyl and citronellyl acetate more effectively than CYP101B1. Overall, we establish that the high selectivity and activity of these enzymes could provide new biocatalytic routes to important fine chemicals.

Introduction

Novosphingobium aromaticivorans DSM12444 is an oligotrophic bacterium first isolated from coastal plain subsurface sediments (at a depth of 410 m below land surface) in the USA [1, 2]. It is hypothesised that the bacterium is capable of using different aromatic hydrocarbons including toluene, *p*-cresol, naphthalene, salicylate and xylenes as the sole carbon and energy source [1]. A large number of genes encoding cytochrome P450 and other monooxygenase or dioxygenase enzymes are found in this bacterium. These enable it to metabolise a wide variety of compounds which allow it to survive in environments that offer little to support life [2]. The genome of this bacterium contains sixteen P450 enzyme-encoding genes [3]. These sixteen P450s belong to ten different families, and among those, four enzymes (B1, C1, D1 and D2) are from the CYP101 family. These, and one other, from the CYP111 family (A2) use a common class I electron transfer system consisting of a flavin-dependent ferredoxin reductase, ArR, and a [2Fe-2S] ferredoxin, Arx [3-5]. Genes of all five cytochrome P450 enzymes have been cloned with these electron transfer partners in an *Escherichia coli* (*E. coli*) host to generate efficient whole-cell biotransformation systems capable of biocatalytic oxidations on a gram per litre scale [3, 6]. Both CYP101D1 and CYP101D2 selectively oxidise (*R*)-camphor to 5-*exo*-hydroxycamphor [3, 6]. Therefore, these enzymes have the same substrate and metabolite profile as the archetypal CYP101A1 ($P450_{cam}$) from the bacterium *Pseudomonas putida* [3, 6-8]. CYP101B1 oxidised camphor but unlike the CYP101A1 and CYP101D enzymes, it was unselective, generating four different products [3, 6]. CYP101B1 exhibited a strong binding affinity for both *α*- and *β*-ionone (≥95% spin-state shift, K_d = 0.23 μM and 0.26 μM, respectively) and displayed high catalytic activity when oxidising these norisoprenoids. This enzyme catalysed the hydroxylation of these substrates on the cyclohexyl ring remote from the butenone side chain to generate the 3-hydroxy metabolites with high regioselectivity [9].

When screened with other monoterpenoids, CYP101B1 was found to be capable of biocatalytic oxidation, but the level of product formation activity and selectivity were lower when compared to norisoprenoids [10]. For instance, CYP101B1 catalysed the oxidation of (+)-fenchone to generate three hydroxylated metabolites with low product formation activity compared to *α*- and *β*-ionone [10]. It was hypothesised that the butenone side chain of the norisoprenoid substrates holds these molecules in place for efficient and selective oxidation. Subsequently, monoterpenoid oxidation was improved by converting the terpenoids into their acetate ester derivatives [10]. For example, CYP101B1 catalysed the oxidation of monoterpenoid esters such as myrtenyl acetate, bornyl acetate

Department of Chemistry, University of Adelaide, Adelaide, SA, 5005, Australia
E-mail: stephen.bell@adelaide.edu.au
Electronic Supplementary Information (ESI) available: [substrate binding data, gas chromatography, mass spectrometry and NMR data]. See DOI: 10.1039/x0xx00000x

View Article Online DOI: 10.1039/D0CY01045F

and fenchyl acetate with high product formation activities and selectivity [10]. This confirmed that this carbonyl group was a key feature which enables the oxidation reactions to proceed with high catalytic activity, turnover number and coupling efficiency [9].

The last CYP101 family enzyme from *N. aromaticivorans*, CYP101C1, displays little activity for camphor oxidation but like CYP101B1 can oxidise norisoprenoid substrates [3, 11]. For example *β*-ionone is oxidised with high activity [3, 11]. While CYP101C1 oxidised *β*-ionone to the same metabolites as CYP101B1, the selectivity was different. The major metabolite for CYP101C1 arises from C4 (75%) hydroxylation while CYP101B1 oxidised the substrate predominantly at the C3 (90%) position [11]. An interesting feature of CYP101C1 activity is that high rates of catalytic oxidation are observed despite only marginal changes in the heme spin-state shift upon substrate binding [11]. This is in contrast to the behaviour of CYP101A1, CYP101B1 and other P450s in which a substrate induced shift of the enzyme to the ferric high-spin form is an excellent indicator of the enzyme activity [9, 12-18].

Alicyclic molecules, which constitute a large class of organic compounds including monocyclic cycloalkanes, cycloalkanones and cycloalkyl esters, are used in manufacturing perfumes, flavours, essential oils, tobacco products, herbicides, insecticides and serve as intermediates in the pharmaceutical industry [19]. They are commonly used as solvents and found as secondary metabolites in microbes and plants, with terpenoids being particularly prevalent [19-22]. Functionalisation of the C-H bonds of alicyclic compounds would have an enormous impact on the field of chemical synthesis [23-26]. Indeed, selective C-H bond activations could pave the way for preparing complex functionalised molecular skeletons [27-31]. Selective late stage C-H bond functionalisation is one of the most challenging chemical processes due to the low reactivity of the bond and overoxidation issues [26, 32]. The selective hydroxylation of alicyclic hydrocarbons using mild conditions would simplify many processes in synthetic chemistry [32, 33]. Metal catalysts and oxidising reagents oxidise the inert C-H bonds of alicyclic compounds [34-38]. For instance, cyclohexanone and cyclohexanol, which are essential chemical intermediates for the synthesis of polyamide and plastics, are synthesised using cyclohexane oxidation processes including H_2O_2-based hydroxylation, Au-Pd bimetallic catalysts and homogeneous transition-metal salt catalysts which are designed to reduce the occurrence of overoxidation products [26, 39-41]. However, despite an enormous effort over the last few decades, challenges remain [32]. The main concern is that harsh chemicals, heavy metals and toxic solvents are used in most of these chemical oxidation approaches [42].

The use of a selective or even an enantioselective enzyme biocatalyst instead of the toxic chemical catalyst could be an alternative and efficient approach to avoid the issues discussed above. Bacterial and fungal species can oxidise the C-H bonds of cyclic compounds [22, 43-50].

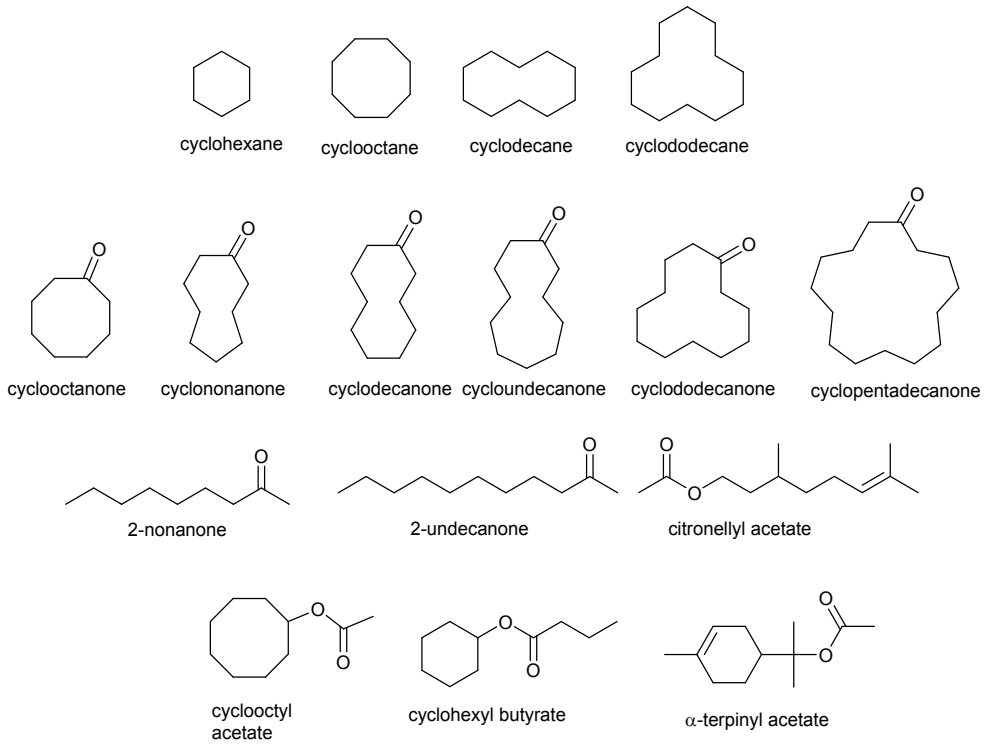

Figure 1 Substrates tested with CYP101B1 and CYP101C1 during the course of this work.

For example, Fonken *et al.* reported the oxidation of C12-, C13- and C14- macrocyclic compounds using *Sporotrichum sulfurescens* (*Beauveria sulfurescens* ATCC7159) and Ashton *et al.* described the oxidation of cyclododecanone and cyclopentadecanone by different fungi such as *Calonectria decora*, *Daedalea rufescens*, *Ophiobolus herpotrichus* and *Rhizopus nigricans* [51, 52]. Self-sufficient P450 BM3 and some of its mutants have been reported to oxidise C8-C12 cycloalkanes [53]. However, in most of the above oxidations of cyclic and linear alkane derivatives the product formation activity or selectivity was low.

CYP101B1 is a highly efficient biocatalyst for the oxidation of monoterpenoid acetates and adamantyl esters [9, 10, 54]. With these bicyclic and tricyclic substrates the regioselectivity of oxidation was high and the site of C-H bond abstraction by CYP101B1 was on the opposite side of the ring system to the ester group. This is in agreement with the regioselectivity of norisoprenoid oxidation by CYP101B1. With this in mind, we investigated a series of cyclic substrates, ranging in ring size from 6 to 15 carbons including their alcohol ester and ketone derivatives, with CYP101B1 (Figure 1). In addition, given the modified regioselectivity observed for CYP101C1 catalysed oxidation of *β*-ionone, these substrates were also assessed with this enzyme to determine if different reactivity and selectivity are observed.

Results

The oxidation of cyclic alkanes by CYP101B1 and CYP101C1

The spin-state induced by substrate binding to a P450 provides a measure of the ability of the molecule to displace the aqua ligand bound to the heme iron. This is corroboration that the substrate fits into the active site in a position suitable for C-H bond abstraction. Previously, none of the substrates which have been investigated with CYP101C1 have induced a substantial change of the spin-state from the low spin form (all <20% high spin; HS) [11]. Similar results were observed here with all the substrate assessed showing a < 20% HS (data not shown). The spin-state shift of CYP101B1 was analysed with each substrate and demonstrated greater variability (Table 1). Cyclohexane, cyclooctane, cyclodecane and cyclododecane induced a shift in the spin-state of CYP101B1 within the range of 15% to 40% high spin (Table S1; henceforth % will be assigned to the proportion of high spin (HS) heme-induced by substrate binding). This indicates that these hydrocarbon substrates are not able to displace the 6th ferric-aqua ligand of CYP101B1 as well as the norisoprenoids (≥ 95%). The substrate binding affinity of cyclodecane and cyclododecane were high with low dissociation constants K_d = 0.88 ± 0.04 μM and K_d = 0.16 ± 0.03 μM, respectively. Cyclooctane bound with the enzyme more weakly (K_d = 31 ± 4 μM, Table S1, Figure S1) [14].

The NADH oxidation and product formation rates (PFR) can be used as a measure of P450 biocatalytic activity. These were low for CYP101B1 with cyclohexane, cyclodecane and cyclododecane (PFR; 2 to 42 nmol.(nmol-P450)$^{-1}$.min^{-1}; henceforth abbreviated to min^{-1}; Figure 2, Table S1). The coupling efficiency, which is the productive use of reducing equivalents for oxidised metabolite formation, was also minimal (3 to 11%; Table S1). Addition of cyclooctane to CYP101B1 induced a five-fold higher PFR (209 ± 17 min^{-1}; Table S1) than that observed with the next best substrate; cyclodecane. The higher levels of product can be attributed to a significant increase in the coupling efficiency (49%; Table S1). CYP101C1 displayed lower product formation activity than CYP101B1 with all of these cycloalkanes (Figure 2, Table S1).

Previously we have demonstrated that modification of an active site histidine residue (H85) in CYP101B1 can alter the substrate preference of this enzyme [55]. Therefore, we tested the H85F mutant of CYP101B1, with cyclic alkanes. Use of the mutated variant resulted in improved binding parameters with cyclooctane and cyclodecane. This translated into an increase in the NADH oxidation activity of both by CYP101B1. However, only the PFR activity with cyclooctane was improved to any significant degree (282 ± 23 min^{-1}, Table S1).

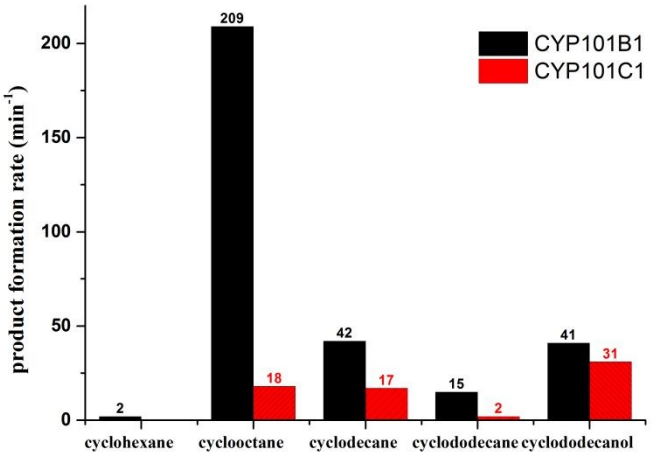

Figure 2 The overall product formation rates of CYP101B1 and CYP101C1 with cyclic alkanes and alcohols. Product formation rates are given in nmol.nmol-CYP^{-1}.min^{-1}. Further details are provided Table S1 in the Supporting Information.

The conversion of the majority of the cycloalkanes by both enzymes and the CYP101B1 H85F variant yielded a single metabolite. In most cases the metabolites were identified by a GC coelution experiment with authentic standards of the cycloalkanols (Figure S2). Cyclooctane and cyclodecane generated the cycloalkanol as the major product. Minor products were confirmed as the cycloketone by GC-MS coelution experiment with an authentic standard (Figure S2). The ketone further oxidation product was most abundant in the oxidation of cyclododecane by CYP101C1 (25% versus 5% for CYP101B1). The CYP101B1 catalysed turnover of cyclooctane resulted in the largest total turnover number (TTN; 3400 ± 150, Table S1).

The oxidation activity of the larger cyclododecane was significantly lower than for the C8 and C10 cycloalkanes with CYP101C1, CYP101B1 and even for the H85F variant of CYP101B1 (best PFR of 15 min^{-1}, Table S1). Both enzymes catalysed the oxidation of cyclododecane to generate the same major metabolite (92% for CYP101B1 and 60% for CYP101C1) alongside two minor products. The major metabolite, as detected in the GC-MS analyses of the *in vitro* turnovers of both

enzymes, did not coelute with a cyclododecanol standard. We then demonstrated that cyclododecanol is a better substrate, in terms of binding and oxidation activity, than the parent cycloalkane for both enzymes (Figure 2, Table S1). Analysis and scale up of these turnovers enabled the identification of the major metabolite as 1,7-cyclododecanediol (Figure S2). CYP101B1 was more selective and generated greater quantities of this diol as the major product (Figure S2). Minor metabolites were assigned as 1,6-cyclododecanediol and either the other diastereomer of 1,6-cyclododecanediol or 1,4-cyclododecanediol based on their ^{13}C NMR signals [14]. Therefore both enzymes convert the cyclododecane into cyclododecanol, which is then further oxidised to the diols reported above. Neither enzyme showed any activity with cyclohexanol and cyclooctanol. Overall CYP101C1 and CYP101B1 are capable of metabolising cycloalkanes, with the latter displaying higher product formation activity.

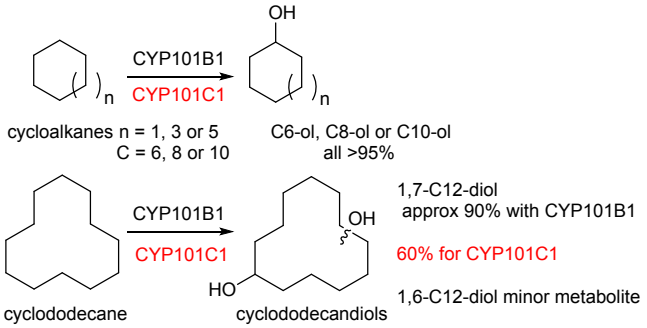

Scheme 1 The oxidation of cycloalkanes by CYP101B1 and CYP101C1. Note cyclodecane oxidation by CYP101C1 resulted in a greater extent of further oxidation to cyclodecanone (25%) than CYP101B1 (Figure S2).

The oxidation of ketones by CYP101B1 and CYP101C1

Next cycloalkanones were screened with both enzymes to explore how the binding affinity and catalytic activity would be altered for substrates which contain a ketone moiety. Cyclooctanone induced a 10% heme spin-state shift in CYP101B1 (Table 1). Both enzymes displayed low activity, and there was no evidence of any product formation with cyclooctanone. Addition of the larger cyclononanone shifted the heme spin-state of CYP101B1 to 30% high spin (Figure S1). The dissociation constant (K_d) of CYP101B1 with cyclononanone was 46 ± 21 μM (Figure S1 and Table 1). The PFRs with CYP101B1 and CYP101C1 were 131 min^{-1} and 75 min^{-1}, respectively (Table 1). The greater PFR of CYP101B1, was predominantly due to the greater coupling efficiency of reducing equivalents to product formation (Table 1). This was also reflected in a greater total turnover number for CYP101B1 (TTN 886 versus 226).

The GC analyses of the *in vitro* turnovers of CYP101B1 and CYP101C1 with cyclononanone highlighted that these enzymes catalysed the oxidation of this substrate with different regioselectivity (Scheme 2 and Figure S2). Whole-cell turnovers were carried out to generate each metabolite in a quantity sufficient for NMR characterisation. Each product was purified via silica column chromatography and identified by their mass and NMR spectra (Figure S3 and S4). The primary metabolite (98%; at RT 12.2 min) generated by CYP101C1 was 2-hydroxycyclononanone [56]. This was assigned based on the multiplet at 4.28-4.21 (H2) and a distinct signal for -CO**H** proton (C2) at 3.79-3.72 ppm in the ^{1}H NMR, which is observed due to the interaction with C=O (Figure S4 and Table S2) [56]. The mass spectrum also matched that reported in the literature (m^+/z = 156.15; Figure S3) [56]. This product was a minor metabolite in the CYP101B1 catalysed oxidation of cyclononanone (4%; Figure S4). Enantioselective GC analysis of the *in vitro* turnover of CYP101C1 displayed a mixture of 2-hydroxycyclononanone enantiomers in a distribution of approximately 30 to 70% (Figure S2).

The ^{1}H NMR spectrum of the major product from the CYP101B1 *in vivo* turnover (87%; at RT 11.2 min; ~22 mg) had a multiplet signal at δ 4.04-4.17 ppm that would correspond to a -C**H**OR (Figure S4). However, in the ^{13}C spectrum a signal for the substrate ketone (C=O) was not observed and a distinct signal at 100.36 ppm was present instead (Figure S4). The HMBC NMR spectrum showed a strong correlation of this carbon signal (100.36 ppm) to the C**H**OR multiplet in the ^{1}H spectrum, which indicated a cyclisation reaction had occurred (Figure S4 and Table S2). This metabolite could then be assigned as 1-hydroxy-10-oxabicyclo[4.3.1]decane. This would arise from hydroxylation at C5 followed by cyclisation through intramolecular nucleophilic attack of the OH at C5 on the carbonyl group to generate the cyclic hemiacetal [57, 58]. The NMR and mass spectrum were in agreement with those reported in the literature for this compound (m^+/z = 156.15; Figure S3 and Figure S4) [57]. The NMR spectra of this sample displayed signals from a minor metabolite (~9% from the NMR integration of **H**C5(OH) and **H**C5O) with 1-hydroxy-10-oxabicyclo[4.3.1]decane [58]. It was predicted to be 5-hydroxycycloalkanone the precursor to the 1-hydroxy-10-oxabicyclo[4.3.1]decane hemiacetal. This was confirmed by comparing the ^{1}H NMR spectrum peak of H5 at 3.79-3.73 ppm with that reported in the literature (Table S2, Figure S4) [58]. These two species would be present in equilibrium. The minor product from the CYP101C1 turnover coeluted with the primary product, 1-hydroxy-10-oxabicyclo[4.3.1]decane, of CYP101B1 (~2%; at RT 11.2 min, Figure S2).

Addition of cyclodecanone caused a 50% shift to the high spin form in CYP101B1 and its binding affinity (K_d = 46 μM) was similar to that of cyclononanone (Table 1) [14]. Both CYP101C1 and CYP101B1 had higher oxidation activity with this substrate compared to cyclononanone (Table 1). Despite the CYP101C1 system displaying a greater NADH oxidation rate (531 min^{-1} versus 323 min^{-1}), its product formation rate was lower due to a reduced coupling efficiency (22% versus 45%, Table 1). The catalytic oxidation of cyclodecanone by each enzyme formed different monooxygenase products as identified by the GC-MS analyses (m^+/z = 170.2 and m^+/z = 170.1; Figure S3).

View Article Online
DOI: 10.1039/D0CY01040E

Table 1 Substrate binding, turnover and coupling efficiency data for CYP101B1 and CYP101C1 with cycloalkanones. The *in vitro* turnover activities were measured using a ArR:Arx: CYP101B1/CYP101C1 concentration ratio of 1:10:1 (0.5 mM CYP enzyme, 50 mM, pH 7.4). N is the NADH oxidation rate, PFR is the product formation rate, C is the coupling efficiency and TTN the total turnover number. The data are reported as mean ± S.D. (n = 3), and rates (N and PFR) are given in nmol.nmol-CYP^{-1}.min^{-1}. - Not measured or not able to be determined accurately. n.p: no product.

Substrate	CYP101B1/ CYP101C1	HS %	K_d (μM)	N	PFR	C (%)	TTN
cyclooctanone	CYP101B1	-	-	93 ± 9	n.p	n.p	-
	CYP101C1	**-**	**-**	**88 ± 2**	**n.p**	**n.p**	**-**
cyclononanone	CYP101B1	30	46 ± 21	308 ± 10	131 ± 11	43	886 ± 77
	CYP101C1	**-**	**-**	**289 ± 16**	**75 ± 4**	**26**	**226 ± 36**
cyclodecanone	CYP101B1	50	46 ± 2	323 ± 38	149 ± 54	45	1730 ± 50
	CYP101C1	**-**	**-**	**531 ± 75**	**113 ± 13**	**22**	**1180 ± 90**
cycloundecanone	CYP101B1	80	8.4 ± 0.3	409 ± 11	222 ± 14	54	3480 ± 290
	CYP101C1	**-**	**-**	**660 ± 53**	**141 ± 18**	**22**	**3300 ± 330**
cyclododecanone	CYP101B1	90	2.4 ± 0.4	391 ± 11	283 ± 38	72	5750 ± 280
	CYP101C1	**-**	**-**	**853 ± 24**	**239 ± 31**	**28**	**543 ± 62**
cyclopentadecanone	CYP101B1	75	0.5 ± 0.1	126 ± 4	47 ± 3	38	-
	CYP101C1	**-**	**-**	**217 ± 4**	**14 ± 3**	**7**	**-**
2-nonanone	CYP101B1	20	140 ± 10	552 ± 11	219 ± 34	40	5700 ± 80
	CYP101C1	**-**		**270 ± 12**	**92 ± 15**	**34**	**-**
2-undecanone	CYP101B1	30	44 ± 1	568 ± 3	340 ± 50	60	1660 ± 90
	CYP101C1	**-**		**311 ± 12**	**59 ± 25**	**19**	**-**

Previously we have demonstrated that CYP101B1 generated two major metabolites in a 3:2 ratio. A minor metabolite, which eluted earlier than the others, was also formed (Figure S2 and Table S2) [14]. Both major metabolites from CYP101B1 *in vivo* turnovers of cyclodecanone were confirmed as equilibrium mixtures of 1-oxabicyclo[5.3.1]undecan-1-ol and 5-hydroxycyclodecanone and 1-oxabicyclo[6.3.1]undecan-1-ol (~42%) and 6-hydroxycyclodecanone [14, 58]. For CYP101C1, the GC/GC-MS analyses of the turnovers displayed one major metabolite (90%; at RT 7.2 min) which coeluted with the minor product from CYP101B1 oxidation. The minor metabolites of the CYP101C1 turnover coeluted with the major hydroxylated product of CYP101B1 (Figure S2). The major hydroxylated metabolite from CYP101C1 oxidation (m^+/z = 170.2, Figure S3) was purified (~15 mg) and identified as 2-hydroxycyclodecanone by NMR (Figure S4). The ^{1}H NMR spectrum of this metabolite contained two distinct signals for C**H**OH at 4.29-4.17 ppm and CHO**H** at 3.88-3.76 ppm and the ^{13}C NMR signal of the C2 carbon (79.11 ppm) displayed significant deshielding due to its proximity with the carbonyl group [59].

The high spin component of ferric CYP101B1 after the addition of cycloundecanone was greater than that observed with the smaller cyclic ketones (80%; Figure S1 and Table 1). The binding affinity, K_d = 8.4 μM, of this substrate was also 5-fold higher than the smaller substrates (Table 1). Cycloundecanone was oxidised by both enzymes with CYP101C1 exhibiting a faster NADH oxidation rate but oxidation by CYP101B1 occurred with a higher coupling efficiency, 54%, and PFR, 222 ± 14 min^{-1} (Table 1).

The GC-MS analysis of the *in vitro* turnover of CYP101C1 with cycloundecanone revealed a single major hydroxylated product (~92%; RT 8.4 min; m^+/z = 184.40) with three minor metabolites making up the remainder (Figure S2 and Figure S3). The primary metabolite of this substrate was generated and isolated (~20 mg). The product was assigned as 2-hydroxycycloundecanone based on the mass spectrum and the ^{1}H and ^{13}C NMR spectra and comparison with those reported in the literature and above (Figure S4) [60]. Enantioselective-GC analysis showed that two enantiomers of the 2-hydroxycycloundecanone metabolite were generated in almost equal amounts (45:55; Figure S2).

View Article Online
DOI: 10.1039/D0CY01040E

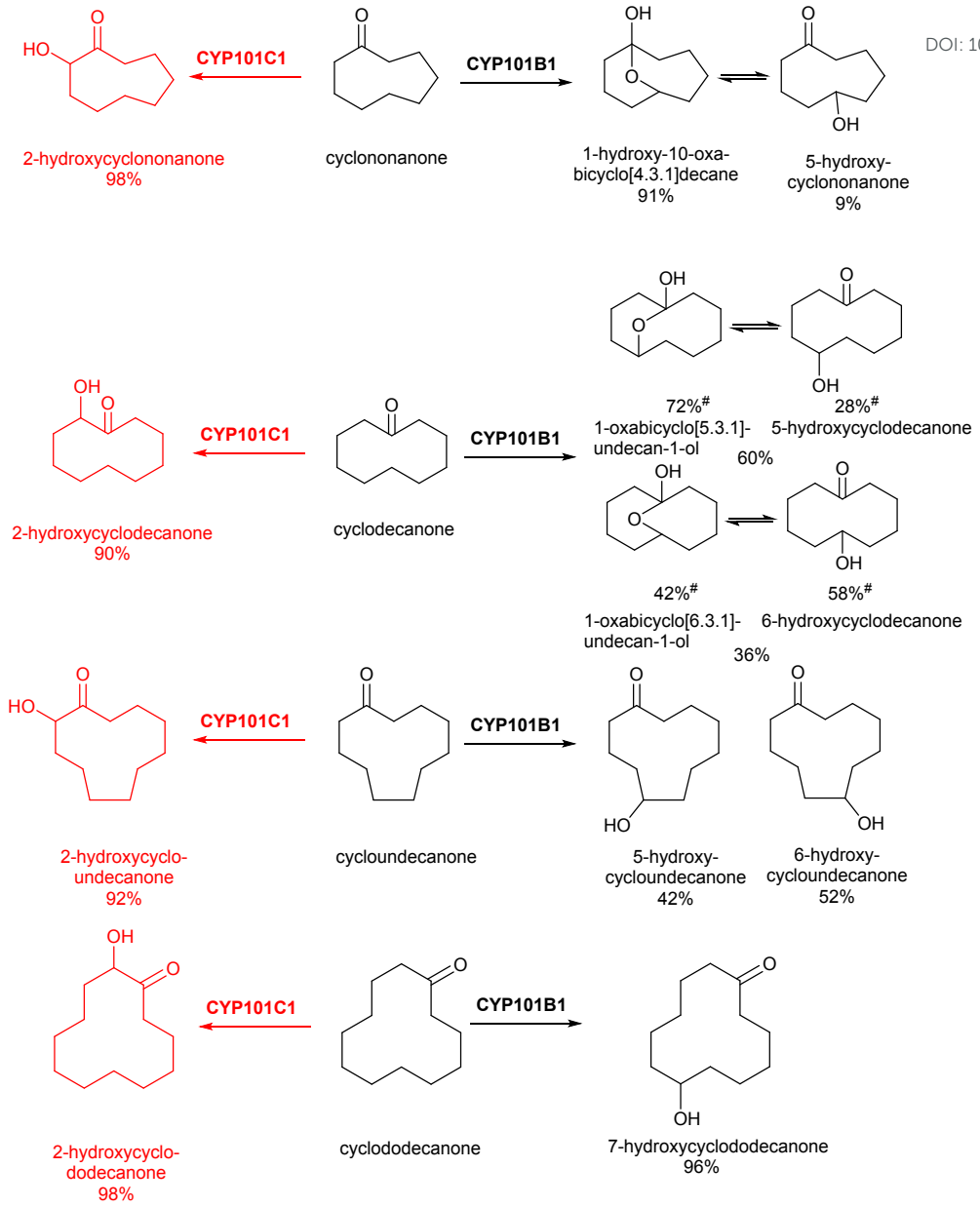

Scheme 2 The oxidation of cyclic ketones by CYP101B1 and CYP101C1. The full selectivity details and the data for cyclopentadecanone are provided in the main text

and SI [14]. # The distributions were obtained from the NMR spectra.

View Article Online
DOI: 10.1039/D0CY01040E

Large scale turnovers of CYP101B1 generated two major metabolites which coelute with the minor metabolites from the CYP101C1 turnover (~42%; 10 mg, m^+/z = 184.30 and ~52%; 15 mg, m^+/z = 184.20, Figure S2). Two minor hydroxylated metabolites were also observed one of which (~3%; RT 8.4 min) coeluted with 2-hydroxycycloundecanone in the GC-MS (Figure S2). Both the major products had multiplet signals in the ^{1}H NMR at 3.76-3.70 and 3.72-3.66 ppm, respectively. These are consistent with hydroxylated products (Figure S4). The correlations in the ^{1}H-^{13}C HMBC NMR spectra, were used to identify these metabolites as 5-hydroxycycloundecanone and 6-hydroxycycloundecanone. Additional minor peaks in the ^{1}H and ^{13}C NMR of this product indicated that another metabolite was also present, but this was not able to be characterised (Figure S4). The remaining minor product, which was generated in low amount, (RT 8.8 min in GC-MS, ≤4%) in both the CYP101B1 and CYP101C1 oxidation reactions was not generated in sufficient quantity for NMR characterisation. The mass spectrum indicated that it was a further oxidation product with a mass, m^+/z = 182.30 (Figure S3). Addition of cyclododecanone shifted the heme spin-state of CYP101B1 almost entirely to the high spin form (90%). This substrate bound even more tightly than cycloundecanone (K_d = 2.4 μM; Table 1 and Figure S1). The PFR of CYP101B1 for cyclododecanone was 283 min^{-1}, and the coupling efficiency was the highest observed across the cycloketones; 72% versus the next best at 54% (Table 1). As a consequence, the total turnover number was significantly greater than for the other cyclic ketones (TTN 5750; Table 1). While CYP101C1 showed an even higher NADH oxidation activity (853 min^{-1}), the PFR and coupling efficiency for the oxidation of this substrate were lower; 239 min^{-1} and 28%, respectively (Table 1).

GC-MS analysis of the oxidation of cyclododecanone by CYP101C1 displayed a single major metabolite (98%; RT 15.5 min) with one other minor product (RT 17.7 min; Figure S2). The mass spectra of these products were consistent with monooxygenase metabolites (m^+/z = 198.25 and m^+/z = 198.05; Figure S3). The primary metabolite of cyclododecanone turnover was generated using the CYP101C1 *in vivo* turnover system and isolated for further characterisation (~29 mg). Consistent with the selectivity of CYP101C1 with the other cyclic ketones this was identified as 2-hydroxycyclododecanone by NMR and a coelution experiment with a commercial standard (Figure S2) [59, 60]. Enantioselective GC analysis revealed that the oxidation of CYP101C1 generated a mixture of 2-hydroxycyclododecanone enantiomers (45%:55%; Figure S2).

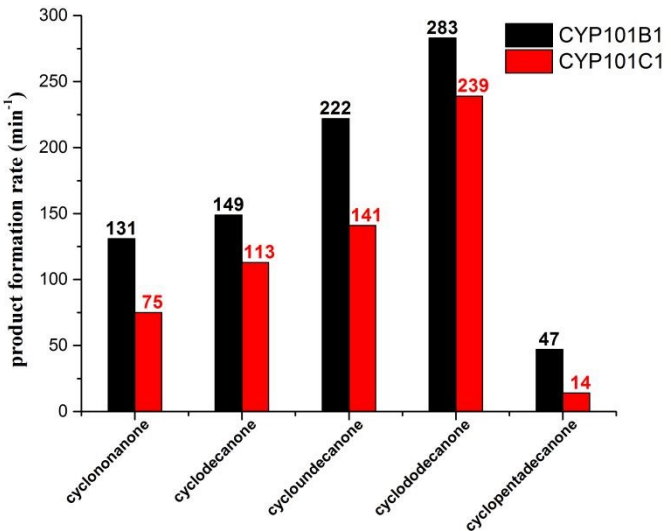

The major product (96%) formed after the oxidation of cyclododecanone by CYP101B1 was isolated (~27 mg, m^+/z = 198.35) and has been identified as 7-hydroxycyclododecanone by NMR analysis [14, 51]. This metabolite coeluted in the GC-MS analysis with the minor metabolite of the CYP101C1 oxidation, confirming its formation in this reaction (m^+/z = 198.05). A minor metabolite (~4%) from oxidation by CYP101B1 was unable to be generated in a large enough quantity for characterisation by NMR. However, the mass spectrum was consistent with a monooxygenase product with a mass of, m^+/z 198.35 (Figure S3).

Figure 3 An overview of product formation rates of CYP101B1 and CYP101C1 with cycloalkanones. Product formation rates are given in nmol.nmol-CYP^{-1}.min^{-1}.

Next we tested the fifteen-carbon ring species cyclopentadecanone to assess if these enzymes could bind and oxidise this larger cyclic ketone whilst maintaining the selectivity of oxidation. This substrate induced a 75% spin-state shift in CYP101B1 and displayed very tight binding to CYP101B1 (K_d = 0.5 μM, Table 1 and Figure S1) demonstrating that the active site of this enzyme can accommodate these larger molecules. CYP101B1 oxidised cyclopentadecanone with a PFR of 47 min^{-1} compared to 14 min^{-1} for CYP101C1 (Table 1). The coupling efficiency of both enzymes was reduced compared to the cyclododecanone oxidations (Table 1). CYP101C1 oxidised this substrate into two metabolites, and GC-MS analysis revealed that both of these were monohydroxylated products (both m^+/z = 240.25, Figure S3). Neither was generated in sufficient quantity for NMR analysis. The primary metabolite (64%; RT 14.6 min) was confirmed by comparing its mass spectrum and fragmentation pattern with the reported mass spectrum of 2-hydroxycyclopentadecanone. This was in agreement with the selectivity of CYP101C1 catalysed oxidation of the other cyclic ketones in this work (Figure S3) [59, 61].

CYP101B1 mediated oxidation of cyclopentadecanone generated a single major hydroxylated product, which was detected in the GC-MS analysis (90%; RT 15.6 min; m^+/z = 240.25; Figure S3). To confirm the identity of the metabolite, it was synthesised in higher amount. In the ^{1}H NMR, a multiplet peak at 3.71-3.64 ppm confirmed the presence of a monohydroxylated product. The ^{13}C NMR suggested the presence of more than one species and the presence of minor metabolites (≤10%; in a total of ~24 mg; Figure S4). HMBC correlations were used to assign the major metabolite as 8-hydroxycyclopentadecanone (Figure S4) [51]. The interactions of the carbonyl carbon (215.30) with H2, H15 (2.47-2.33 ppm) and H3, H14 (1.74-1.60 ppm) were used to determine these proton peaks. C4 (29.64 ppm) and C5 (30.18 ppm) were identified using the HMBC correlations with H2 (2.47-2.33 ppm) and H3 (1.74-1.60 ppm), respectively. C5 (30.18) did not show any interaction with the C**H**(OH) peak (3.71-3.64 ppm), indicating hydroxylation did not occur in C6 or C7. C6 (25.90) was assigned via the correlation of H5 (1.40-1.25), and C6 displayed a weak interaction with the peak at 3.71-3.64 ppm, demonstrating the insertion of oxygen likely occurred at C8 (72.70 ppm; Figure S4). The mass spectrum fragmentation pattern was also in

View Article Online
DOI: 10.1039/D0CY01405

agreement with this assignment (Figure S3) [51]. The 8-hydroxycyclopentadecanone metabolite coeluted with the minor product (36%) from the CYP101C1 oxidation reactions in the GC-MS (Figure S2). There was also a small amount of a further oxidation product (5%) observed in the GC-MS analysis of the CYP101B1 turnovers (m^+/z = 238.20; Figure S3). This minor product was assigned as cyclopentadecane-1,8-dione by comparing its mass spectrum with that reported in the literature (Figure S3) [51]. The enantioselective GC analyses of both CYP101B1 and CYP101C1 *in vitro* turnovers did not display any separation of these metabolites.

To further explore the substrate range of CYP101B1 and CYP101C1 we next assessed if they could oxidise the linear ketones 2-nonanone and 2-undecanone. 2-Nonanone and 2-undecanone induced 20% and 30% heme spin-state shift in CYP101B1, respectively (Figure S1). 2-Nonanone bound with a lower affinity to CYP101B1 than 2-undecanone (140 µM versus 44 µM; Figure S1). These bound more weakly when compared with their cyclic counterparts, cyclononanone and cycloundecanone (Table 1). CYP101B1 oxidised 2-nonanone with a faster NADH oxidation rate (552 min^{-1} versus 270 min^{-1}), PFR (219 min^{-1} versus 92 min^{-1}) and a higher coupling efficiency (40% versus 34%) than CYP101C1 (Table 1). Enzymatic oxidation of 2-nonanone by CYP101B1 generated a single major metabolite accounting for 98% of total turnover products (Figure S2). The mass spectrum (m^+/z = 158.20; Figure S3) and NMR analysis enabled assignment as 8-hydroxy-2-nonanone.

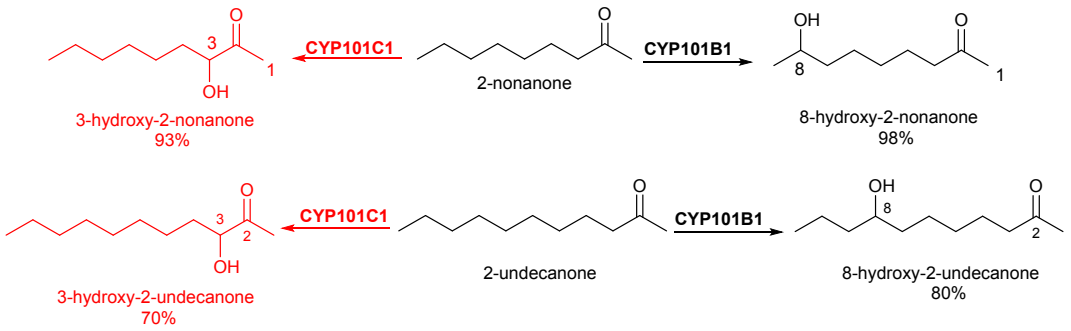

Scheme 3 The oxidation of linear ketones by CYP101B1 and CYP101C1. The selectivity of the major product is given and further details are provided in the main text and SI.

The coupling of H8 (3.86-3.73 ppm) and correlation of C8 (70.71 ppm) with the distinctive doublet peak of the H9 methyl protons at 1.19 ppm being the distinguishing signals (Figure S3 and Scheme 3) [62]. CYP101C1 oxidised 2-nonanone to a different major product (~93%; at RT 8.5 min, m^+/z = 158.65) alongside a minor metabolite, which coeluted with 8-hydroxy-2-nonanone. The major product was not purified in sufficient quantity for NMR analysis but its mass spectrum fragmentation pattern matched that expected of 3-hydroxy-2-nonanone (Figure S3 and Scheme 3).

2-Undecanone was oxidised with a high PFR, 340 min^{-1} and coupling efficiency, 60% (Table 1). CYP101C1 catalysed the oxidation of this substrate with much slower PFR of 59 min^{-1} and a lower coupling efficiency (19%, Table 1). CYP101B1 catalysed oxidation of 2-undecanone was less selective and formed one major product (80%) alongside three minor metabolites (Figure S2 and Scheme 3). The major product (RT 14.95 min, 18 mg) was characterised by NMR (Figure S4). The characteristic multiplet peak at 3.63-3.53 ppm in the ^{1}H NMR spectrum indicated a hydroxylated metabolite which was assigned as 8-hydroxy-2-undecanone due to the interactions of C8 (74.26 ppm) with the protons of 1.52-1.37 ppm (H6, H7, H9 and H10, Figure S4). The minor metabolites (at RT 15.2 min and 15.9 min) were not separated in sufficient amount for NMR identification. However, the ^{13}C NMR of the major metabolite displayed minor carbon signals **C**H(OH) at 75.92 ppm and 74.34 ppm. In the HMBC NMR spectrum, the carbon signal (75.92 ppm) correlated strongly with H11 (0.96-0.88 ppm) and this metabolite was assigned as 9-hydroxy-2-undecanone (Figure S4). The other carbon signal at 74.34 ppm showed the correlation with the protons at 1.52-1.1.28 ppm, and this product was assumed to be 7-hydroxy-2-undecanone based on its retention time and NMR (see supporting information; Figure S3 and S4) [63]. The third minor metabolite at RT 6.2 min was identified by coelution experiment in GC-MS with the main product of CYP101C1 (Figure S2). CYP101C1 metabolised 2-undecanone into three metabolites with a ratio of 70:20:10 (Figure S2). The major metabolite (70%; RT 6.2 min) was assigned as 3-hydroxy-2-undecanone by matching its mass spectrum with the published data (Figure S3 and Scheme 3) [59]. The minor metabolites of CYP101C1 turnovers coeluted with the products of CYP101B1 in GC-MS enabling their assignment (Figure S2 and Scheme 3).

In summary, the oxidative activities of both enzymes were better with the cycloalkanones compared to the cyclic alkanes and alcohols. Substrate profiling indicated that CYP101B1 and CYP101C1 were both able to accommodate and oxidise ketones of varied length and ring size. The cyclic ketones, which were hydroxylated, ranged from C9 to C15. CYP101C1 predominantly hydroxylated the ketones at the C2 (alpha) carbon while CYP101B1 was more selective for C-H bond abstraction at carbons more remote from the carbonyl group with a preference for zeta substitution in linear ketones (and ranging from 5 to 8 carbons depending on the size of the ring).

The oxidation of cyclic esters by CYP101B1 and CYP101C1

We have demonstated that ester directing groups can be used with CYP101B1 to hold a substrate in a suitable position in the active site for efficient and selective oxidation [10, 14, 54, 64]. In order to assess if a directing group could improve the catalytic activity

View Article Online
DOI: 10.1039/D0CY01040E

and selectivity of both enzymes, different ester derivatives of a selection of alcohols were investigated with CYP101C1 (Figure 1). The oxidation of the majority of the substrates by CYP101B1 and CYP101C1 generated the same major metabolite [14]. However, CYP101C1 catalysed these reactions with lower activity, coupling efficiency and TTN (Table 2, Table S3). The oxidation of these cyclic compounds with ester substituents by CYP101B1 and CYP101C1 occurred predominantly at the C-H bonds on the opposite side of the ring to the ester group, for example, C4 for cyclohexyl derivatives, and C5, and C7 for the cyclooctyl and cyclododecyl derivatives, respectively (Figure S2 and S4) [14]. For most substrates both enzymes favoured formation of the *trans* diastereomer, however, for 7-hydroxycyclododecyl acetate CYP101C1 preferentially generated another metabolite which has previously been postulated to be the *cis* isomer (Figure S2 and S4) [14].

α-Terpinyl acetate, which contains a *p*-menthane backbone was also screened to assess the effect of the presence of a double bond in the ring and the addition of a methyl group, on the activity and selectivity of both enzymes. Oxidation of *α*-terpinyl acetate by CYP101C1 proceeded with a significantly higher NADH oxidation rate than that measured for CYP101B1 (898 min^{-1} versus 178 min^{-1}; Table 2). No product was detected in the GC-MS analysis of the *in vitro* turnover of this substrate with CYP101B1. However, CYP101C1 oxidised the *α*-terpinyl acetate with a product formation rate of 497 min^{-1} and a coupling efficiency of 55% (Table 2). The GC analysis of the CYP101C1 *in vitro* turnover revealed a primary (82%) alongside a minor metabolite (Figure S2). The epoxide of *α*-terpinyl acetate was synthesised by *m*-chloroperbenzoic acid using a standard method [65]. However, this did not coelute with the metabolite generated by CYP101C1 (at RT 15.25 min in GC-MS).

Table 2 Substrate binding, turnover and coupling efficiency data for CYP101B1 and CYP101C1 with selected substrates containing the ester directing group [14]. The turnover activities were measured as described in Table 1. The data are reported as mean ± S.D. (n = 3). Rates are given in nmol.nmol-CYP^{-1}.min^{-1}. - not measured or not able to be determined accurately. n.p no product. Additional data provided in Table S3.

Substrate	CYP101B1/ CYP101C1	N	PFR	Coupling (%)	TTN
cyclohexyl acetate	CYP101B1	415 ± 56	56 ± 6	14	910 ± 385
	CYP101C1	**173 ± 13**	**n.p**	**-**	**-**
cyclohexyl butyrate	CYP101B1	603 ± 32	310 ± 62	51	9580 ± 530
	CYP101C1	**188 ± 16**	**25 ± 10**	**13**	**741 ± 48**
methylcyclohexyl acetate	CYP101B1	736 ± 26	261 ± 20	34	9460 ± 540
	CYP101C1	**257 ± 8**	**36 ± 11**	**14**	**288 ± 21**
cyclooctyl acetate	CYP101B1	722 ± 16	223 ± 20	31	8180 ± 1100
	CYP101C1	**961 ± 23**	**268 ± 24**	**28**	**3330 ± 690**
cyclododecyl acetate	CYP101B1	394 ± 8	94 ± 7	23	2990 ± 770
	CYP101C1	**587 ± 7**	**50 ± 8**	**9**	**797 ± 100**
α-terpinyl acetate	CYP101B1	178 ± 20	-	-	-
	CYP101C1	**898 ± 16**	**497 ± 20**	**55**	**2810 ± 160**
citronellyl acetate	CYP101B1	418 ± 4	115 ± 1	28	-
	CYP101C1	**654 ± 8**	**304 ± 11**	**47**	**1540 ± 220**

The major metabolite was generated in the required quantity for characterisation (~10 mg). The presence of a signal at 4.20 ppm in ^{1}H NMR confirmed a hydroxylated metabolite (Figure S4). The NMR and correlations of the proton signals in the ^{1}H-^{1}H gCOSY and HSQC NMR were used to identify the metabolite as 3-cyclohexene-1-methanol, 5-hydroxy-*α*,*α*,4-trimethyl-,*α*-acetate (Figure S4). The signal at 71.25 ppm (C5) in the ^{13}C NMR spectrum of the primary product displayed a correlation with (H7) in the HMBC NMR, and the presence of the two alkene carbons peaks, were in agreement with this assignment (Figure S4).

A minor metabolite (at RT 12.5 min) was not generated in high enough quantity for NMR characterisation. The spectrum of the major metabolite contained additional signals that could be assigned to either the other diastereomer of the major product or result from hydrolysis of the ester (to yield sobrerol; Figure S4) [66, 67]. The stereochemistry of the major metabolite could not be assigned from the NMR spectra (Figure S4).

CYP101C1 also catalysed the oxidation of the linear ester citronellyl acetate with a significantly faster PFR activity and coupling efficiency than CYP101B1 (Table 2). GC analysis revealed that a single product was generated in both the CYP101B1 and CYP101C1 *in vitro* turnovers of citronellyl acetate

Journal Name ARTICLE
View Article Online
DOI: 10.1039/D0CY01040E

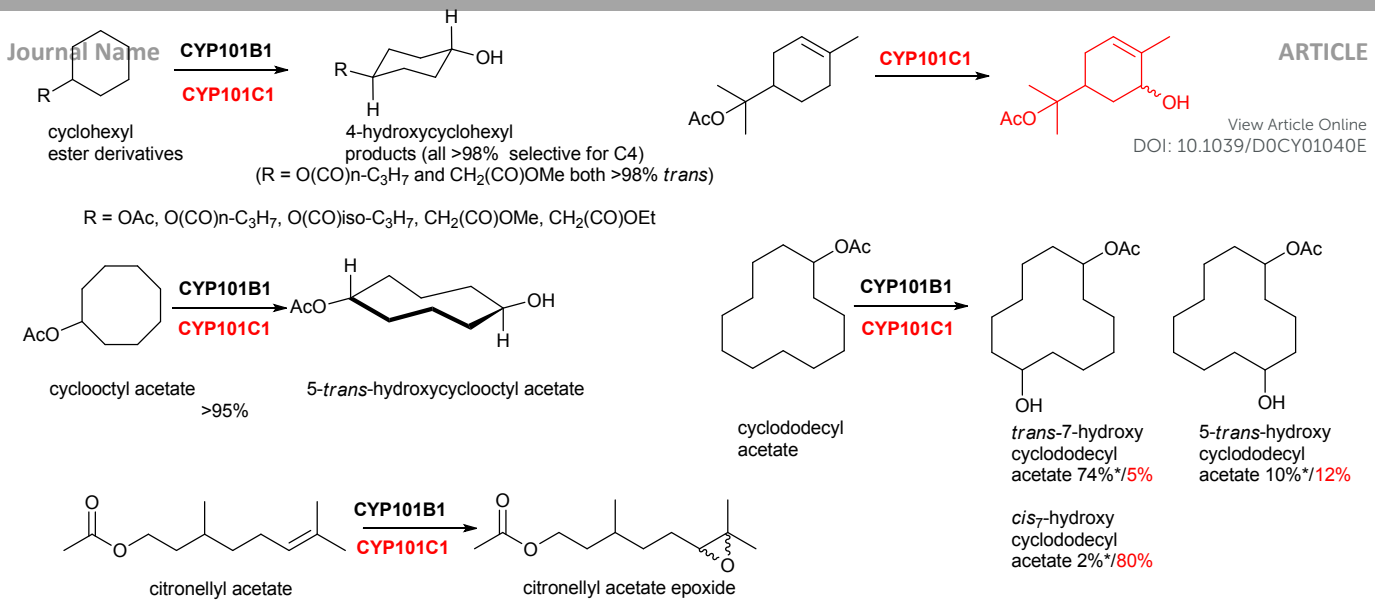

(Figure S2). The product was confirmed as citronellyl acetate epoxide by matching the GC retention time and mass spectra with a standard, which was synthesised via the oxidation of citronellyl acetate with *m*-chloroperbenzoic acid (Figure S2 and S3) [65].

Discussion

CYP101B1 and CYP101C1 exhibited low oxidation and product formation activities with cyclic alkanes (C_6 to C_{12}) but both enzymes were able to oxidise these substrates. The larger cyclic alkanes cyclooctane, cyclodecane and cyclododecane bound better to CYP101B1 than did cyclohexane. The product formation rates for both enzymes with these larger substrates were also improved compared to that of cyclohexane. One major hydroxylated product alongside a small amount of ketone further oxidation metabolite was detected in the turnovers after oxidation of the cycloalkanes by these enzymes. The majority of the cyclic alcohols did not show any significant binding affinity with CYP101B1 and CYP101C1, and little or no product formation was observed. The exception was cyclododecanol, which was oxidised by both enzymes and generated the 1,7-cyclododecanediol metabolite as the major product. Cycloalkanones (C_9 to C_{15}) induced higher spin-state shifts in the CYP101B1 compared to their cyclic alkanes and alcohol equivalents. With these substrates, CYP101B1 displayed faster product formation rates than the CYP101C1.

Scheme 4 The oxidation of cycloalkyl and terpenoid esters by CYP101B1 and CYP101C1 [14]. If not indicated the stereochemistry could not be assigned by NMR or enantiomers were not separated using enantioselective GC.

The oxidation activity was highest with cycloundecanone and cyclododecanone. CYP101B1 oxidised cyclononanone and cyclodecanone yielding 1-hydroxy-10-oxabicyclo[4.3.1]decane, 1-oxabicyclo[5.3.1]undecan-1-ol and 1-oxabicyclo[6.3.1]undecan-1-ol. These exist in a transannular tautomeric equilibrium with their corresponding hydroxy cycloalkanones.

The regioselectivity of CYP101C1 oxidation with these cyclic ketones was different, and it generated the 2-hydroxy metabolites as the major product irrespective of the size of the ring. The regioselectivity for larger cycloalkanones like cyclododecanone and cyclopentadecanone, where the hydroxylation occurs predominantly on the remote site of the ring to the ketone moiety with CYP101B1 or at C2 with CYP101C1 is promising for future applications requiring the selective oxidation of these or similar substrates. The improved activity of CYP101B1 and CYP101C1 with these cycloalkanone structures is likely due to the presence of the ketone moiety. This enabled improved substrate binding to the enzyme active site and therefore more efficient turnover. Linear ketones were also oxidised with low to moderate activity by CYP101B1. CYP101B1 oxidised 2-nonanone and 2-undecanone predominantly at the C8 position while the 3-hydroxy metabolite was the major product observed after oxidation by CYP101C1.

The binding orientation of these ketone in CYP101B1 and CYP101C1 must be significantly altered to account for observed regioselectivity differences. Of relevance here is that the CYP101C1 structure displays significant changes compared to the other known CYP101 family members [11]. These include the presence of additional loops and short helices and a distinctive active site [4, 11, 68]. This is in line with the altered substrate range of this enzyme. Compared to the active site of P450cam, CYP101D1 and CYP101D2, CYP101C1 replaces the hydrophilic tyrosine, which hydrogen bonds to the camphor carbonyl group, with a more hydrophobic methioine residue [4, 11, 68, 69]. There is currently no structural data for the CYP101B1 enzyme to help explain how the substrates are bound. CYP101B1 is functionally different from all of the enzymes mentioned above which suggests that its structure, especially around the active site, will not closely resemble the others. Based on the substrate range we would expect that the structure of CYP101B1 may be more similar to that of CYP101C1. Using sequence alignments highlights that in CYP101B1 a histidine residue replaces the tyrosine (in CYP101A1, CYP101D1 and CYP101D2) and methionine (in CYP101C1). As this is more hydrophobic than the

methionine at the equivalent position in CYP101C1 we hypothesise that this change, along with others in the active site, would contribute to the different binding orientation of the cycloalkanones in CYP101B1 and CYP101C1.

Cyclic compounds containing ester directing groups were also oxidised by CYP101B1 and CYP101C1. For example, cyclohexanol derivatised with butyrate directing groups were efficiently oxidised by CYP101B1. CYP101C1 was able to oxidise the majority of these substrates, but the catalytic performance was lower due to the poor productive utilisation of the reducing equivalents compared to the CYP101B1 system. In the case of α-terpinyl acetate, which has additional functional group complexity to the six membered cyclohexyl ring, CYP101B1 did not generate any oxygenated metabolites while CYP101C1 oxidised this substrate more effectively. α-Terpinyl acetate, which was supplied as a mixture of enantiomers, was oxidised at the C5 position. The substrates containing an ester directing groups were oxidised regioselectively on a carbon on the opposite side of the ring (*trans*-isomer) by CYP101B1 and CYP101C1. In contrast to the cyclic esters CYP101C1 epoxidised citronellyl acetate to the epoxide with higher activity than the CYP101B1 system.

The regioselectivity achieved for cyclic alkanes, ketones and esters are impressive given the lack of other distinguishing features on these cyclic molecules. Further optimisation is required to enhance the stereoselectivity of oxidation. This could be achieved through protein engineering. Previously high selectivity and turnovers have been reported for oxidation of bicyclic, tricyclic and fused ring systems [44, 49, 50]. However, the CYP101B1 and CYP101C1 enzymes catalysed the oxidation of larger ring compounds containing a ketone moiety or ester directing group with high regio- and stereoselectively. The high product formation rates and TTNs (up to 9500) for the optimal substrates combined with the levels of selectivity are favourable compared to other systems. For example, the PikC monooxygenase system from *Streptomyces venezuelae* oxidises cyclic substrates including cycloalkyls, macrolides and macrolactones substituted with desosamine or dimethylamine containing anchoring groups with TTN up to 500 [70, 71]. With the PikC monooxygenase system the addition of double bonds or other functional groups to the larger ring structures tended to improve the selectivity of the oxidations. The selectivity of the PikC sytem was reduced for cycloalkyl substrates compared to more functionalised macrolides and macrolactones; e.g., 7 products were generated with the protected cyclododecanol but the oxidation of narbomycin to pikromycin is regioselective [70-73]. CYP101B1 and CYP101C1 would be excellent enzymes to target for the oxidation of other natural products which contain large cyclic ring systems. The activity and selectivity of the CYP102A1 (P450Bm3) catalysed oxidation of cembrenoid derivatives has also been reported. Multiple rounds of mutagenesis and substrate engineering resulted in the formation multiple products at allylic and non-activated C-H bonds but more saturated analogues displayed lower activity and selectivity [74-76].

Experimental

View Article Online
DOI: 10.1039/D0CY01040E

General reagents, substrates and solvents were purchased from Sigma-Aldrich, Tokyo Chemical Industry (TCI), Alfa-Aesar and Acros-Organics. Antibiotics and other molecular biology reagents were supplied by Astral Scientific (Australia). The methods used to prepare, purify and analyse all the enzymes (CYP101B1 and CYP101C1) and proteins (the electron transfer partners; ArR and Arx) in this study were performed as described previously [11, 14, 54, 55]. The substrate binding and the *in vitro* and whole-cell oxidation reactions were performed using the methods described previously [14].

UV/Vis spectroscopy was performed on Varian Cary 60 or 5000 spectrophotometers, and these assays were maintained at 30 ± 0.5 °C by an attached Peltier unit [14]. Gas Chromatography-Mass Spectrometry (GC-MS) was performed using a DB5(ms) column in a Shimadzu GC-17A instrument attached to a QP5050A MS detector or a Shimadzu GC-2010 coupled to a GC-MS-QP2010S detector (EI positive ion mode). Gas Chromatography (GC) analyses were performed on a Shimadzu Tracera GC coupled to Barrier Discharge Ionization Detector, equipped with either a Supelcowax (Supelco, 30 m x 0.32 mm x 0.25 µm) or a RT®-BDEXse chiral silica column (Restek; 30 m x 0.32 mm x 0.25 µm). The GC methods have been described in detail previously [14]. NMR spectra were acquired on an Agilent DD2 or a Varian Inova spectrometer, operating at 500 or 600 MHz for 1H and 126 or 151 MHz for 13C. A combination of ^{1}H, ^{13}C, COSY, HSQC, HMBC and ROESY experiments were used to determine the structure of the metabolites.

Conclusions

The cytochrome P450 monooxygenase enzymes CYP101B1 and CYP101C1, when combined with the electron transfer partners, Arx and ArR can efficiently oxidise cyclic hydrocarbon derivatives. The C-H bond abstraction and selectivity of oxidation for a given methylene group was high and the metabolites could be generated in good quantity. Therefore these P450 enzymes are excellent candidates for further study to generate biocatalysts for the selective functionalisation of more complex substrates. They are also an excellent starting point for developing more stereoselective oxidations of these substrates. The ability to catalyse the oxidation of a range of cyclic and linear compounds highlights the potential of these two enzymes to insert an oxygen atom into inert C-H bonds. Overall, cyclic ketones and esters were good substrates for CYP101B1 and CYP101C1. The improved product formation activity and coupling efficiencies of CYP101B1 and CYP101C1 with cycloketones compared to the equivalent cycloalkanes illustrates that the addition of a carbonyl group plays an important role in enhancing substrate binding and biocatalysis. The work on CYP101B1 demonstrates that the enzyme must hold the substrate in a way that selective C-H bond abstraction occurs on the ring at a position remote to the carbonyl functionality. With CYP101B1 there is also a good correlation with the substrate binding parameters and the activity. Further investigation of larger (>C15) and smaller (<C6) cyclic and linear

compounds with ketone and ester moieties would be valuable to expand their substrate range. Lactones and lactams, e.g. *ε*-caprolactone, *ε*-caprolactam, pentadecanolide and 16-hexadecanolide, which have received attention because of their chemical versatility, could be investigated with these monooxygenase enzymes. Protein engineering of both enzymes could be a useful approach to improve the binding affinity and selectivity further for efficient late stage functionalisation of alkane derived natural products.

Conflicts of interest

"There are no conflicts to declare".

Acknowledgements

We thank the University of Adelaide for financial support. Md.R.S. thanks the University of Adelaide for an International PhD scholarship.

Notes and references

[a] Current address; Department of Pharmaceutical Technology, University of Dhaka, Dhaka, Bangladesh.

1. J. Fredrickson, F. Brockman, D. Workman, S. Li and T. Stevens, *Appl. Environ. Microbiol.*, 1991, **57**, 796-803.
2. J. Fredrickson, D. Balkwill, G. Drake, M. Romine, D. Ringelberg and D. White, *Appl. Environ. Microbiol.*, 1995, **61**, 1917-1922.
3. S. G. Bell and L. L. Wong, *Biochem. Biophys. Res. Commun.*, 2007, **360**, 666-672.
4. W. Yang, S. G. Bell, H. Wang, W. Zhou, N. Hoskins, A. Dale, M. Bartlam, L. L. Wong and Z. Rao, *J. Biol. Chem.*, 2010, **285**, 27372-27384.
5. S. G. Bell, W. Yang, J. A. Yorke, W. Zhou, H. Wang, J. Harmer, R. Copley, A. Zhang, R. Zhou, M. Bartlam, Z. Rao and L. L. Wong, *Acta Crystallogr. D,* 2012, **68**, 277-291.
6. S. G. Bell, A. Dale, N. H. Rees and L. L. Wong, *Appl. Microbiol. Biotechnol.*, 2010, **86**, 163-175.
7. M. H. Gelb, D. C. Heimbrook, P. Malkonen and S. G. Sligar, *Biochemistry*, 1982, **21**, 370-377.
8. I. C. Gunsalus and G. C. Wagner, *Methods Enzymol.*, 1978, **52**, 166-188.
9. E. A. Hall and S. G. Bell, *RSC Adv.*, 2015, **5**, 5762-5773.
10. E. A. Hall, M. R. Sarkar, J. H. Z. Lee, S. D. Munday and S. G. Bell, *ACS Catal.*, 2016, **6**, 6306-6317.
11. M. Ma, S. G. Bell, W. Yang, Y. Hao, N. H. Rees, M. Bartlam, W. Zhou, L. L. Wong and Z. Rao, *ChemBioChem*, 2011, **12**, 88-99.
12. M. T. Fisher and S. G. Sligar, *J. Am. Chem. Soc.*, 1985, **107**, 5018-5019.
13. S. G. Sligar and I. C. Gunsalus, *Proc. Natl. Acad. Sci. U. S. A.*, 1976, **73**, 1078-1082.
14. M. R. Sarkar, S. Dasgupta, S. M. Pyke and S. G. Bell, *Chem. Commun.*, 2019, **55**, 5029-5032.
15. J. E. Stok, K. E. Slessor, A. J. Farlow, D. B. Hawkes and J. J. De Voss, in *Monooxygenase, Peroxidase and Peroxygenase Properties and Mechanisms of Cytochrome P450*, eds. E. G. Hrycay and S. M. Bandiera, Springer International Publishing, Cham, 2015, DOI: 10.1007/978-3-319-16009-2_12, pp. 319-339.
16. S. G. Bell, R. Zhou, W. Yang, A. B. Tan, A. S. Gentleman, L. L. Wong and W. Zhou, *Chemistry*, 2012, **18**, 16677-16688.
17. T. Coleman, S. H. Wong, M. N. Podgorski, J. B. Bruning, J. J. De Voss and S. G. Bell, *ACS Catal.*, 2018, **8**, 5915-5927.
18. M. N. Podgorski, T. Coleman, R. R. Chao, J. J. De Voss, J. B. Bruning and S. G. Bell, *J. Inorg. Biochem.*, 2020, **203**, 110913.
19. Q. Cheng, S. Thomas and P. Rouviere, *Appl. Microbiol. Biotechnol.*, 2002, **58**, 704-711.
20. P. Morgan and R. J. Watkinson, in *Biochemistry of microbial degradation*, ed. C. Ratledge, Springer Netherlands, Dordrecht, 1994, DOI: 10.1007/978-94-011-1687-9_1, pp. 1-31.
21. K. Kostichka, S. M. Thomas, K. J. Gibson, V. Nagarajan and Q. Cheng, *J. Bacteriol.*, 2001, **183**, 6478-6486.
22. H. Iwaki, S. Wang, S. Grosse, H. Bergeron, A. Nagahashi, J. Lertvorachon, J. Yang, Y. Konishi, Y. Hasegawa and P. C. Lau, *Appl. Environ. Microbiol.*, 2006, **72**, 2707-2720.
23. A. E. Shilov and G. B. Shul'pin, *Chem. Rev.*, 1997, **97**, 2879-2932.
24. F. Kakiuchi and S. Murai, in *Activation of Unreactive Bonds and Organic Synthesis*, Springer, 1999, pp. 47-79.
25. C. Jia, T. Kitamura and Y. Fujiwara, *Acc. Chem. Res.*, 2001, **34**, 633-639.
26. J. Long, H. Liu, S. Wu, S. Liao and Y. Li, *ACS Catal.*, 2013, **3**, 647-654.
27. A. D. Aloise, M. E. Layton and M. D. Shair, *J. Am. Chem. Soc.*, 2000, **122**, 12610-12611.
28. T. Newhouse and P. S. Baran, *Angew. Chem. Int. Ed.* , 2011, **50**, 3362-3374.
29. T. Seiser, O. A. Roth and N. Cramer, *Angew. Chem.*, 2009, **121**, 6438-6441.
30. M. S. Chen and M. C. White, *Science*, 2007, **318**, 783-787.
31. M. C. White and J. Zhao, *J. Am. Chem. Soc.*, 2018, **140**, 13988-14009.
32. R. Curci, L. D'Accolti and C. Fusco, *Acc. Chem. Res.*, 2006, **39**, 1-9.
33. K. I. Goldberg and A. S. Goldman, *Activation and functionalization of C-H bonds*, American Chemical Society Washington, DC, 2004.
34. P. J. Figiel, A. M. Kirillov, M. F. C. G. da Silva, J. Lasri and A. J. Pombeiro, *Dalton Trans.*, 2010, **39**, 9879-9888.
35. P. J. Figiel, A. M. Kirillov, Y. Y. Karabach, M. N. Kopylovich and A. J. Pombeiro, *J. Mol. Catal. A: Chemical*, 2009, **305**, 178-182.
36. M. V. Kirillova, Y. N. Kozlov, L. S. Shul'pina, O. Y. Lyakin, A. M. Kirillov, E. P. Talsi, A. J. Pombeiro and G. B. Shul'pin, *J. Catal.*, 2009, **268**, 26-38.
37. M. V. Kirillova, A. M. Kirillov, M. L. Kuznetsov, J. A. Silva, J. J. F. da Silva and A. J. Pombeiro, *Chem. Commun.*, 2009, 2353-2355.
38. A. M. Kirillov, M. V. Kirillova, L. S. Shul'pina, P. J. Figiel, K. R. Gruenwald, M. F. C. G. da Silva, M. Haukka, A. J. Pombeiro and G. B. Shul'pin, *J. Mol. Catal. A: Chemical*, 2011, **350**, 26-34.
39. K. Kamata, K. Yonehara, Y. Nakagawa, K. Uehara and N. Mizuno, *Nat. Chem.*, 2010, **2**, 478.
40. R. G. Bergman, *Nature*, 2007, **446**, 391.
41. U. Schuchardt, W. A. Carvalho and E. V. Spinacé, *Synlett*, 1993, **1993**, 713-718.

42. T. J. Collins, *Acc. Chem. Res.*, 2002, **35**, 782-790.
43. R. Fasan, *ACS Catal.*, 2012, **2**, 647-666.
44. K. Zhang, S. El Damaty and R. Fasan, *J. Am. Chem. Soc.*, 2011, **133**, 3242-3245.
45. K. Zhang, B. M. Shafer, M. D. Demars, 2nd, H. A. Stern and R. Fasan, *J. Am. Chem. Soc.*, 2012, **134**, 18695-18704.
46. A. Glieder, E. T. Farinas and F. H. Arnold, *Nature biotechnology*, 2002, **20**, 1135-1139.
47. J. C. Lewis, S. M. Mantovani, Y. Fu, C. D. Snow, R. S. Komor, C. H. Wong and F. H. Arnold, *ChemBioChem*, 2010, **11**, 2502-2505.
48. M. W. Peters, P. Meinhold, A. Glieder and F. H. Arnold, *J. Am. Chem. Soc.*, 2003, **125**, 13442-13450.
49. F. Li, X. Zhang and H. Renata, *Curr. Opin. Chem. Biol.*, 2019, **49**, 25-32.
50. J. Li, F. Li, E. King-Smith and H. Renata, *Nat. Chem.*, 2020, **12**, 173-179.
51. M. J. Ashton, A. S. Bailey and E. R. Jones, *J. Chem. Soc. Perkin Trans. 1*, 1974, 1665-1669.
52. G. S. Fonken, M. E. Herr, H. C. Murray and L. M. Reineke, *J. Am. Chem. Soc.*, 1967, **89**, 672-675.
53. E. Weber, A. Seifert, M. Antonovici, C. Geinitz, J. Pleiss and V. B. Urlacher, *Chem. Commun.*, 2011, **47**, 944-946.
54. M. R. Sarkar, E. A. Hall, S. Dasgupta and S. G. Bell, *ChemistrySelect*, 2016, **1**, 6700-6707.
55. M. R. Sarkar, J. H. Z. Lee and S. G. Bell, *ChemBioChem*, 2017, **18**, 2119-2128.
56. E. Friedrich and W. Lutz, *Chem. Ber.*, 1980, **113**, 1245 - 1263.
57. G. A. Molander and J. A. McKie, *J. Org. Chem.*, 1993, **58**, 7216-7227.
58. G. Kräme, A. Oehlhof and H. Meier, *Z. Naturforsc. B*, 2009, **64**, 847.
59. W. Chai, A. Takeda, M. Hara, S.-J. Ji and C. A. Horiuchi, *Tetrahedron*, 2005, **61**, 2453-2463.
60. S. Matsubara, K. Takai and H. Nozaki, *B. Chem. Soc. Jpn*, 1983, **56**, 2029-2032.
61. L. Yu, X. Li, S. Liu, G. Xu and Y. Liang, *J. Sep. Sci.*, 2009, **32**, 3457-3465.
62. H. L. Holland, A. Kohl, B. G. Larsen, P. Andreana and J.-X. Gu, *J. Mol. Catal. B: Enzym.*, 1997, **2**, L253-L255.
63. T. Yagi, T. Hatano, F. Fukui and S. Fukui, *J. Ferment. Bioengineer.*, 1992, **74**, 218-221.
64. M. R. Sarkar, S. D. Houston, G. P. Savage, C. M. Williams, E. H. Krenske, S. G. Bell and J. J. De Voss, *J. Am. Chem. Soc.*, 2019, **141**, 19688-19699.
65. M. Bezard, A.-T. Karlberg, J. Montelius and J.-P. Lepoittevin, *Chem. Res. Toxicol.*, 1997, **10**, 987-993.
66. K. A. da Silva Rocha, J. L. Hoehne and E. V. Gusevskaya, *Chem. Eur. J.*, 2008, **14**, 6166-6172.
67. J. Wolinsky and M. K. Vogel, *J. Org. Chem.*, 1977, **42**, 249-253.
68. W. Yang, S. G. Bell, H. Wang, W. Zhou, M. Bartlam, L. L. Wong and Z. Rao, *Biochemical J.*, 2011, **433**, 85-93.
69. T. L. Poulos, B. C. Finzel and A. J. Howard, *J. Mol. Biol.*, 1987, **195**, 687-700.
70. A. R. Narayan, G. Jimenez-Oses, P. Liu, S. Negretti, W. Zhao, M. M. Gilbert, R. O. Ramabhadran, Y. F. Yang, L. R. Furan, Z. Li, L. M. Podust, J. Montgomery, K. N. Houk and D. H. Sherman, *Nat. Chem.*, 2015, **7**, 653-660.
71. S. Negretti, A. R. Narayan, K. C. Chiou, P. M. Kells, J. L. Stachowski, D. A. Hansen, L. M. Podust, J. Montgomery and D. H. Sherman, *J. Am. Chem. Soc.*, 2014, **136**, 4901-4904.
72. M. M. Gilbert, M. D. DeMars, 2nd, S. Yang, J. M. Grandner, S. Wang, H. Wang, A. R. H. Narayan, D. H. Sherman, K. N. Houk and J. Montgomery, *ACS Cent. Sci.*, 2017, **3**, 1304-1310.
73. S. Li, M. R. Chaulagain, A. R. Knauff, L. M. Podust, J. Montgomery and D. H. Sherman, *Proc. Natl. Acad. Sci. U. S. A.*, 2009, **106**, 18463-18468.
74. P. Le-Huu, T. Heidt, B. Claasen, S. Laschat and V. B. Urlacher, *ACS Catal.*, 2015, **5**, 1772-1780.
75. P. Le-Huu, D. Petrović, B. Strodel and V. B. Urlacher, *ChemCatChem*, 2016, **8**, 3755-3761.
76. P. Le-Huu, D. Rekow, C. Kruger, A. Bokel, T. Heidt, S. Schaubach, B. Claasen, S. Holzel, W. Frey, S. Laschat and V. B. Urlacher, *Chemistry*, 2018, **24**, 12010-12021.

View Article Online
DOI: 10.1039/D0CY01040E

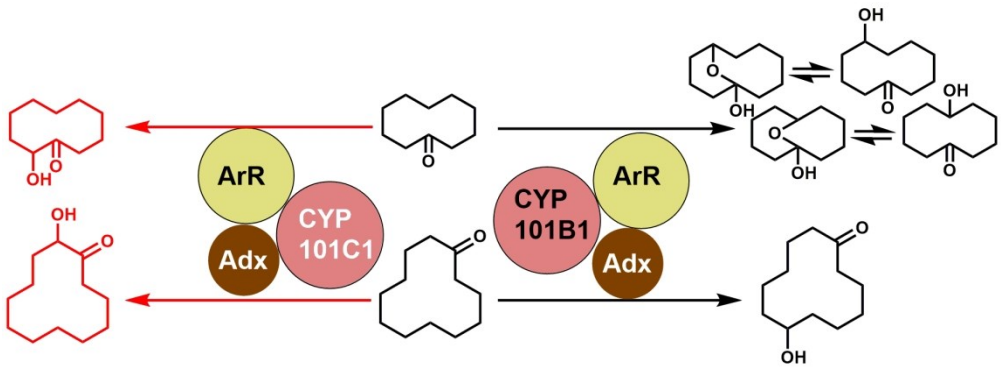

161x59mm (300 x 300 DPI)